Evaluation of Salt Matrix and Organic Additives in Solution Anode Glow Discharge Optical Emission Spectrometry: Taking Silver, Cadmium and Mercury as Examples

Zhaoqing Cai[a, b] and Zheng Wang[a, b, *]

[a] Shanghai Institute of Ceramics, Chinese Academy of Sciences, Shanghai 201899, P. R. China

[b] Center of Materials Science and Optoelectronics Engineering, University of Chinese Academy of Sciences, Beijing 100049, P. R. China

Received: *September 01, 2023;* ***Revised:*** *November 08, 2023;* ***Accepted:*** *November 18, 2023;* ***Available online:*** *November 18, 2023.*

DOI: 10.46770/AS.2023.190

ABSTRACT: The effects of several common interfering elements, low-molecular weight organic compounds (LMWOCs), and surfactants on the analytical performance of solution anode glow discharge optical emission spectrometry (SAGD-OES) were extensively studied. The resistance to interfering elements (Na, K, Mg and Ca) of different analytes (Ag, Cd and Hg) varied wildly. At extremely low concentrations of 1 mg L^{-1}, Ag and Cd signals were suppressed by 31-38% and 17-30%, respectively; however, even at up to 100 mg L^{-1} Na/K/Mg/Ca, the method exhibited satisfactory recovery rates of 91-96% for Hg measurement. These findings give references for the quantitative methods directed against different test elements. The LMW alcohols (methanol and ethanol) and carboxylic acids (formic acid, acetic acid, and propionic acid) added to solution anode exhibited complex and diverse behaviors. Signal suppression was present for Ag, while characteristic emission was enhanced in the case of Hg. Surfactants such as Triton X series gave better results in spectral pattern and analyte response, with a sensitivity increase of 1.4-3.3 times and a notable descent in background levels. Furthermore, the experimental results suggested that the Triton X-100 still improved the detection limits (DLs) and signal-to-back ratios (SBRs) of elements in samples with a certain salinity of 500 mg L^{-1} Na. Despite the presence of Na-rich matrix, the DLs of Ag, Cd and Hg were quite low (1.0, 0.9 and 7 μg L^{-1}, respectively), comparable to various microdischarge spectroscopy methods and ICP-OES.

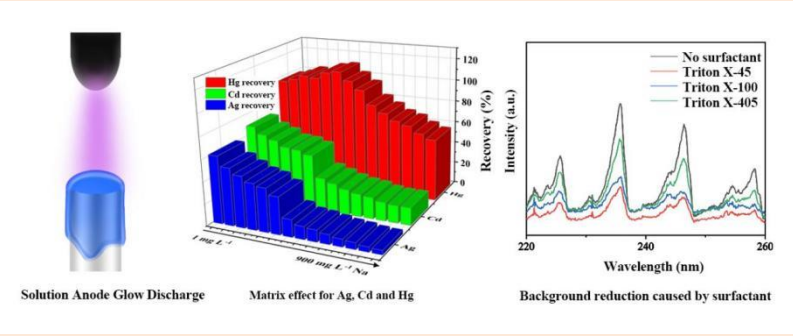

INTRODUCTION

Mature quantitative analysis methods of trace elements in liquid samples such as atomic absorption spectrometry (AAS), hydride generation-atomic fluorescence spectrometry (HG-AFS), inductively coupled plasma-optical emission spectrometry/mass spectrometry (ICP-OES/MS) typically serve as benchmark methods. Although these methods allow the effective determination with high sensitivity, high accuracy, and wide linearity range, they are mainly used in laboratories rather than in the field due to significant analytical support, *e.g.*, high power. Recently, microplasmas have attracted increased attention as alternative excitation sources for OES because of their numerous advantages, including small footprint and low operating cost related to energy and gas consumption.[1-3] Such plasmas include, but are not limited to, solution cathode/anode glow discharge (SCGD/SAGD),[4-11] atmospheric pressure glow discharge (APGD),[12-16] dielectric barrier discharge (DBD)[17-18] and point discharge (PD).[19-24] Among these techniques, SCGD/SAGD exhibits unique advantages in aqueous solution analysis since liquid samples can be introduced into discharge cells to directly act

as electrodes, without additional configuration for nebulization or vapor generation.

As early as 1993, Cserfalvi *et al*.[25-26] proposed a closed SCGD set-up, which was at first termed electrolyte-cathode atmospheric glow discharge (ELCAD), with appealing detection capabilities in the sub-μg mL^{-1} range for many elements. In contrast, SAGD began acting as an excitation source for spectrochemical analysis much later, and the emission of excited atoms of dissolved metals could not be observed at the early stage. In 2016, two research groups independently observed the emission of metal atoms from the flowing liquid anode (FLA) glow discharge plasma, making leap in the application of SAGD in atomic spectroscopy.[5, 27] Encouragingly, detection sensitivity with at least one order of magnitude enhancement was obtained using such SAGD systems in comparison to SCGD-OES. Elements amenable to determination by SAGD, however, are mainly limited to a specific group, namely Ag, Bi, Cd, Hg, In, Pb, Tl and Zn.[4-6, 28] Until recently, Yang and Cai *et al*.[29-31] developed a novel SAGD excitation source maintained in hydrogen-doped atmosphere, extending quantifiable elements scope to hydride forming elements Sb and As.

SAGD-OES device is typically equipped with inert gas and/or cathode (metal electrode) refrigeration, which ensures sufficient discharge stability and signal strength but compromises miniaturization and portability.[28] Yuan *et al*.[6] proposed a simplified design of SAGD-OES without cooling device and inert gas environment. Yu *et al*.[32] used platinum instead of consumable graphite and tungsten electrode materials to improve discharge stability, data repeatability and electrode viability. Despite the improvement of portability, stability and sensitivity by the continuous innovation of SAGD source structure, the interference caused by coexisting ions cannot be neglected in the actual sample analysis.[5, 28, 33, 34] The emission from majority elements was dramatically suppressed in the presence of interfering ions with a concentration of 0.24 mmol L^{-1}.[33] Greda *et al*.[33, 34] carried out a lot of research on the minimization of matrix effects, and the recovery of analyte was found to be advanced by using masking agents and antioxidants, but to a limited extent.

LMWOCs[35-37] and surfactants including non-ionic[38] (such as Triton X-45, Triton X-100) or ionic surfactants[39] (cetyltrimethylammonium chloride, CTAC) are used to treat the solution cathode to fulfill the intensified emission of element in SCGD-OES method. The beneficial effects of LMWOCs are also observed in the SAGD-OES analysis procedure, but are limited to the electrolyte anode at a specific pH value, and vary with the type of additives and metal elements; the responses of In and Bi are greatly promoted and suppressed respectively, for example.[4, 40-42] To the best of our knowledge, no report has been made so far to deal with how surfactants affect the analyte emission of SAGD. Recently, Zhang *et al*.[43] reported the ineffectiveness, even negativity of organic small molecules when analyzing high-salinity samples (3.5 g L^{-1} NaCl) using the SCGD-OES method. Therefore, what might improve the analytical performance of SAGD-OES is now being researched, as well as whether the additive is effective in high salt environments.

New insights into coexisting inorganic salts, as well as chemicals introduced for sample solution modification, is of great value for the SAGD-OES analysis of actual samples, and can supply references for sample pretreatment. Accordingly, it is proposed to thoroughly investigate the matrix effects induced by different salinity (mainly alkali metals and alkaline earth metals, with concentrations ranging from 1 to 900 mg L^{-1}; anions are nitrates) on the quantification of metal elements (taking Ag, Cd and Hg as examples, given their widespread industrial application and strong biological toxicity), and to objectively evaluate the effect of organic small molecules and surfactants (Triton X series). Furthermore, the influence of additives in the presence of sodium matrix is also discussed.

EXPERIMENTAL

Instrumentation. The proposed SAGD-OES device was presented with simplified design, as shown in Fig.1. No inert gas environment or electrode cooling block was contained, and the discharge cell in this case closely resembled the structure of Wang's SCGD.[44] The tapered tungsten (W) rod (ø=2.6 mm) acted as the cathode, and the flowing electrolyte served as the anode. The electrolyte continuously overflowed from the orifice of the quartz capillary (ø in/out=0.38/1.1 mm) which was coaxial with the W rod and 3 mm below it. The capillary was inserted from the hole drilled on the graphite rod (ø=5 mm) and perpendicular to the graphite rod. They were also fixed at the bottom and side of the polytetrafluoroethylene (PTFE) base simultaneously. The graphite rod and W rod were connected to the positive and negative terminals of the power supply (HSPY-600, Hansheng Puyuan

Fig. 1 Schematic diagram of SAGD-OES system.

Technology Beijing Co., Ltd., China) respectively. A ballast resistor (R=2.5 kΩ) was inserted in the circuit to stabilize the current and prevent the transition from glow discharge to arc discharge. The post-discharge liquid was removed from the waste outlet on the PTFE base. Peristaltic pump (BT100-1 L, Lange Constant Flow Pump, Baoding, China) was used to secure the transportation of sample solution and waste liquid. A chain sinnet junction, also known as a daisy chain, was applied in the sampling pipeline to alleviate the pulse fluctuations of the peristaltic pump. The distance between the metal electrode and the solution surface can be shortened instantaneously by squeezing the plastic elastic air pocket in the sampling pipeline, to realize air breakdown and plasma ignition.

The optical radiation from SAGD was focused on the optical fiber probe (QP600 -1-XSR, Ocean Optics Co., Ltd., USA) by a plane-convex lens (f=50 mm, OLB25-050, China) and coupled to the entrance slit (100 μm) of the micro spectrometer (Maya 2000 pro, Ocean Optics Co., Ltd., USA, spectral range 190-409 nm, spectral resolution of 0.35 nm). The optical fiber probe was installed on the platform equipped with three orthogonal micrometer spiral gauges, which can be adjusted accurately in the x, y and z directions, for the purpose of collecting the light radiation of the analyte to the maximum extent. The integration time was set to 300 ms for the atomic lines of Ag, Cd and Hg (Ag I at 338.28 nm, Cd I at 228.80 nm and Hg I at 253.65 nm).

Reagent and sample. All reagents used were of the analytical grade or higher. The deionized water (18.25 MΩ·cm, resistivity) used in the whole experiment was from the ELGA water purification system (PURELAB Classic, UK). The stock standard solutions of Ag (I), Cd (II) and Hg (II) (1000 mg L^{-1}) were provided by the National Iron and Steel Material Testing Center (Beijing, China). Nitric acid (HNO_3, 68 wt%), formic acid (HCOOH, 98 wt%), acetic acid (CH_3COOH, 99.5 wt%), propionic acid (CH_3CH_2COOH, 99.5 wt%), methanol (CH_3OH, 99.5 wt%) and ethanol (CH_3CH_2OH, 99.7 wt%) were all provided by Sinopharm Chemical Reagents Co., Ltd. (Shanghai, China). Triton X-45 [$C_{14}H_{22}(C_2H_4O)_{4.5}$], Triton X-100 [$C_{14}H_{22}O(C_2H_4O)_{9.5}$], and a 70% water solution of Triton X-405 [$C_{14}H_{22}O(C_2H_4O)_{40}$] were purchased from Sigma-Aldrich. The salt matrix effect study was carried out by dissolving an appropriate amount of nitrate of the following elements: K, Na, Mg and Ca (Sigma-Aldrich). The pH value of the solution was measured with a pH meter (PHS-3E, INESA, China).

RESULTS AND DISCUSSION

Effect of experimental parameters (solution pH, discharge current and solution flow rate). Considering that the SAGD cell proposed here differed from the previous designs, key parameters such as solution pH, discharge current and solution flow rate were optimized afresh to get optimal analytical performance. Analyte response is positively correlated with the solution pH value (Fig. 2a), which means that high levels of H^+ (exist as H_3O^+ in solution) hinders the element detection. This could be attributed to the elimination of solvated electrons caused by the excessive H_3O^+ ions[30]. However, the process of increasing pH is also accompanied by the lowering of conductivity, rendering unstable discharge at pH 2.2 and above. To ensure discharge stability while considering the minimal difference in signals between pH 2 and pH 2.2, pH 2 was thus chosen. Within the tested current region, the analyte response trends to rising along with the current increased, as can be seen in Fig. 2b. Our previous work combining SAGD as a vapor generation technique with ICP-OES has shown enhanced signals for Hg and Cd with higher discharge currents[42], indicating that increasing the current promotes the liquid-plasma transport of the analyte. Furthermore, higher current also enhances the atomization and excitation capability of plasma. But practically the effects are limited. When the threshold is reached, there is a

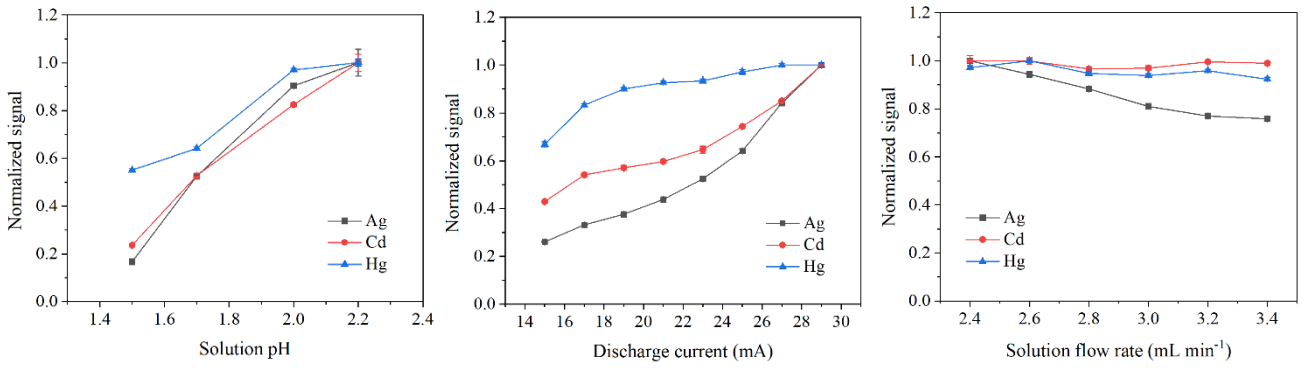

Fig. 2 Effect of solution pH (a), discharge current (b) and solution flow rate (c) on Ag detection (338.28 nm, black line), Cd detection (228.80 nm, red line) and Hg detection (253.65 nm, blue line) in the SAGD-OES system.

trade-off between current, discharge stability and electrode service life—increasing current typically sacrifices others. Therefore, 25 mA was selected for subsequent experiments. Element responses were found to be less susceptible to varying flow rate than solution pH and current, especially for Hg and Cd (Fig. 2c). Slight solution fluctuation does not affect the accuracy of the method/instrument for cadmium and mercury quantification in practical application. However, the rise of flow rate caused a slight decline of Ag signal. According to Greda *et al*.,[45] the vapor generation efficiency of Ag is more susceptible (negatively correlated) to the sample flow rate compared to Hg and Cd. It is thus speculated that the attenuation of Ag radiation may be attributed to the depression in the yield of volatile silver-containing substance. Excessively low flow rate compromises ease of ignition, therefore, 2.8 mL min^{-1} was selected.

The influence of salinity. Na^+, K^+, Mg^{2+} and Ca^{2+} were selected for salt matrix effect test by the fact that these elements are usually found in samples in more abundant quantities than other coexisting metal ions. The corresponding nitrate solids, namely $NaNO_3$, KNO_3, $Mg(NO_3)_2{\cdot}6H_2O$, and $Ca(NO_3)_2{\cdot}4H_2O$, were dissolved in nitric acid solution (pH=2) to prepare the single standard solutions with the above ion concentrations of 100, 200, 300, 400, 500, 700, 900 mg L^{-1}. These standard solutions were diluted with nitric acid solution (pH=2) to lower concentrations such as 1, 2, 3, 4, 5, 10, 50 mg L^{-1}. Single standard solution of Ag, Cd and Hg were added to the above solutions and finally a series of solutions containing different concentrations of Na^+, K^+, Mg^{2+} or Ca^{2+} and certain concentrations of Ag^+, Cd^{2+} or Hg^{2+} (100 μg L^{-1} Ag/Cd, 1 mg L^{-1} Hg) were prepared and tested.

The results are shown in Fig. 3. The recovery of Ag fell within the range of 4-62%, 6-68%, 22-65% and 5-69% respectively when Na^+, K^+, Mg^{2+} or Ca^{2+} coexisted (Fig. 3a). Cd exhibited slightly better salt tolerance, with recoveries of 16-83% throughout this test. Unfortunately, and obviously, the recovery rates were below 85% even in the presence of 1 mg L^{-1} interfering ion. Therefore, pre-separation and/or enrichment or standard addition method is preferred for Ag and Cd quantification. For Hg, however, the recovery rates reached 57-111%, 58-112%, 53-111% and 54-108%, respectively (Fig. 3c). The satisfactory recoveries (91-96%) were achieved even at interfering ion concentrations of 100 mg L^{-1}. It was therefore apparent that the developed Hg measurement method was to some extent immune to the co-presence of these foreign ions, which is equivalent to the salt resistance level of SCGD-OES. The above reveals the good potential of SAGD for mercury detection.

The T_{rot}(OH) and T_{exc}(H) values calculated by Greda et.al[33] suggested that atomization/excitation conditions were not altered by the presence of interfering ions. This means matrix effect is highly likely, or at least by affecting the liquid phase-gas phase transfer efficiency of the analyte. Therefore, a comparison of the

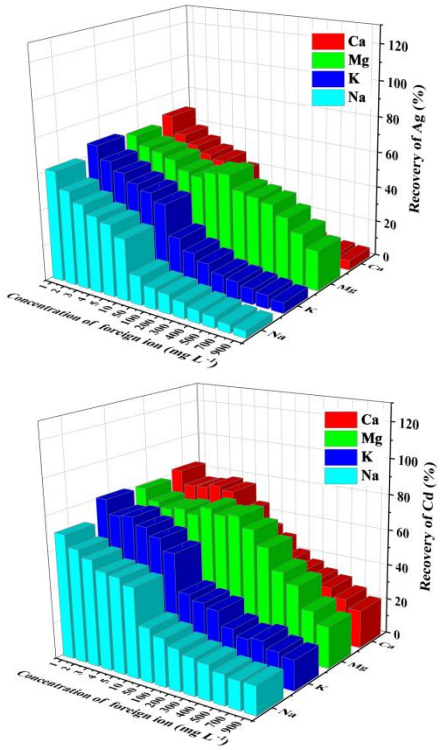

Fig. 3 Effects of coexisting ions on the Ag (a), Cd (b) and Hg (c) emission line intensities (expressed as percent recovery) determined by SAGD-OES.

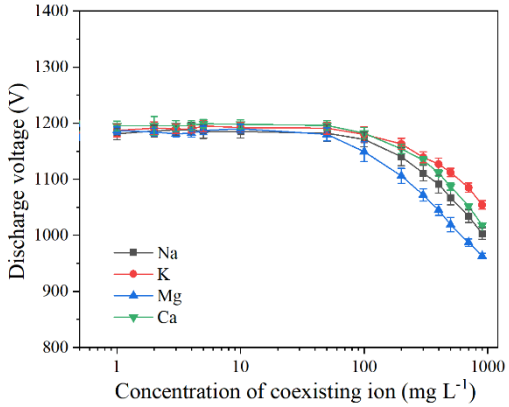

Fig. 4 Effects of coexisting ions on the discharge voltage of the SAGD system generated in contact with HNO_3 solution.

vapor generation efficiency of each element in the SAGD system before and after the addition of matrix (taking natrium salt as an example) was conducted. A closed quartz chamber structure for discharge was designed and employed, maintaining conditions consistent with the open-to-air setup with the exception of the Ar flow rate of 450 mL min^{-1}. The closed SAGD device was coupled with ICP-OES (SAGD-ICP-OES), and the signal strength of ICP-OES was used to assess the alterations in analyte transport efficiency. After the inclusion of the salt matrix, the elements were observed to display a diminishing vapor generation efficiency in the following sequence: Ag, followed by Cd, and finally Hg. This suggests that the higher resistance of the Hg OES signal can be attributed to the stability of the process involved in forming volatile substances of Hg. Notably, regardless of whether the variation in the testing environment was due to the sample matrix or other parameters like discharge current, Hg signals demonstrated the least variability. This could be attributed to the high volatility of Hg as an element, making its volatile compounds readily accessible.

The dependence of the discharge voltage of the SAGD system generated in contact with HNO_3 solution on the concentration of coexisting ion was also measured (Fig. 4). The results show that before the inflection point, *i.e.*, 100 mg L^{-1}, the voltage tends to be constant; after the inflection point, negative correlation exists between the salt concentration and the discharge voltage, which is probably caused by the increase of the conductivity of the solution. This discharge is conducted in constant current (CC) mode, thus lower voltage leads to power reduction. This account for a portion of the decline of analyte response or recovery, especially for mercury—the voltage and the recovery rate have similar variation tendency.

The influence of organic additives. The electrochemical reaction, is considered to be the main mechanism that affects the final spectral response. The role of small organic molecules involved in this process has always been a debatable issue, with great differences among elements.[4, 42] Therefore, the effects of different organic molecules such as formic acid, methanol, acetic acid, ethanol, and propionic acid on the emission intensity of Ag, Cd and Hg were restudied here. A series of Ag, Cd and Hg standard solutions containing 0.05, 0.1, 0.2, 0.5, 1, 2, 5, 7, and 10 wt% of one of the above organic additives were prepared for test. Note that acetic acid and ethanol with a mass fraction of 10% were not in the scope of test because they caused discharge instability.

As shown in Fig. 5a, for the systems with LMWOC concentration beyond 0.2 wt% (0.1 wt% for propionic acid), the Ag signal drops significantly with the increase of the LMWOC concentration. The inhibition rate reached about 80-90%, with the LMWOC concentration up to 2 wt% (5 wt% for methanol). The effect of LMWOCs in the Ag determination by SAGD-OES has been reported with different results. Greda *et al*.[41] found that CH_3OH and C_2H_5OH (0.5%, v/v) significantly inhibited the emission of Ag in the solution at the pH of 2. However, in higher solution acidity (pH 1), the significant increase was observed in the presence of 1 wt% small organic molecules.[40] Since the solution acidity at pH 2 achieved the best performance, our research was completed on this premise, and the conclusions obtained here coincides with those of Greda's report.[41] The decrease of Ag signal in the presence of LMWOCs, perhaps induced by the scavenging of solvated electrons in the liquid phase (the decomposition of organic matter may consume solvated electrons), thus reducing the generation efficiency of volatile substances.[4]

Organic acids and alcohols presented completely different functions on the light radiation of Cd (Fig. 5b). The results reported by Pan *et al*.[46] are roughly similar to our findings. Specifically, formic acid and acetic acid definitely inhibited the generation rate of Cd-containing volatile compounds induced by solution electrode glow discharge (SEGD), while methanol and ethanol boosted the Cd signal. They attributed the enhancement to electrochemical reactions involving reducing species (*e.g.*, e/e_{aq}, H

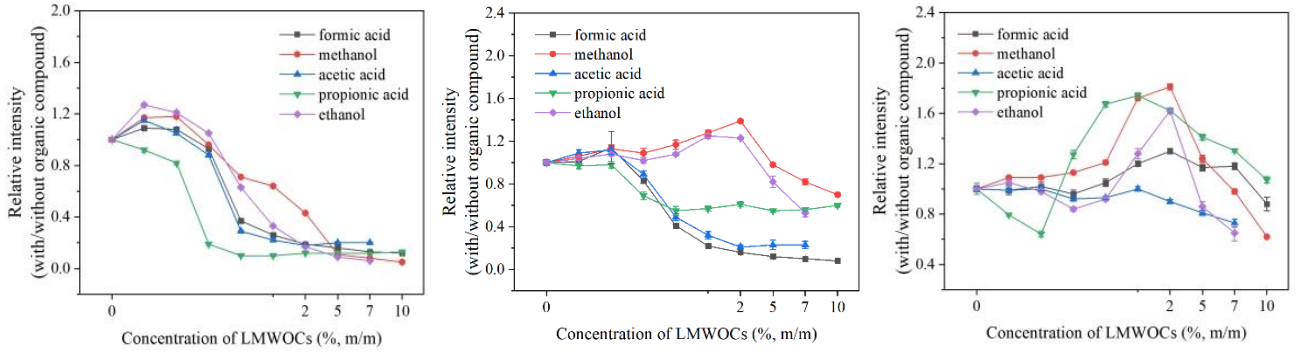

Fig. 5 The relative intensities of Ag (a), Cd (b) and Hg (c) emission lines acquired for sample solutions modified by different LMWOCs at different concentrations. (versus HNO_3, pH 2).

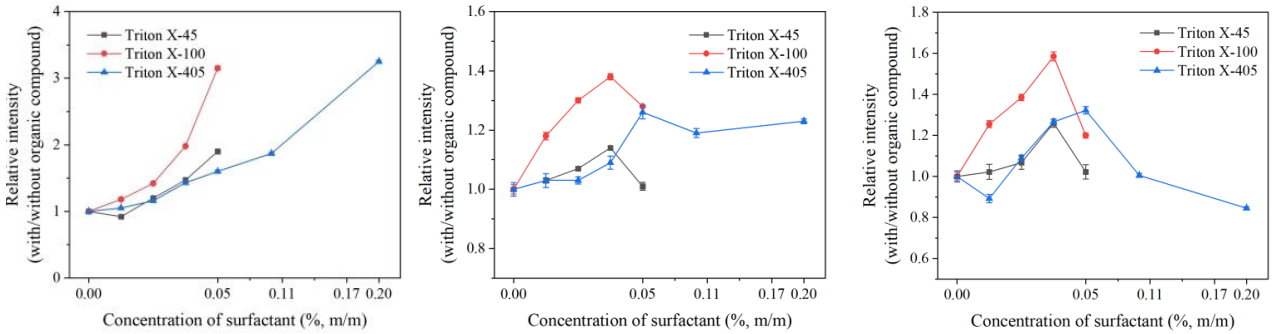

Fig. 6 The relative intensities of Ag (a), Cd (b) and Hg (c) emission lines acquired for sample solutions modified by different surfactant at different concentrations. (versus HNO_3, pH 2).

Fig. 7 The emission spectra of the SAGD system generated in contact with HNO_3 solution containing 0.05 wt% Triton X-405, Triton X-100 and Triton X-45 or without surfactant.

and CH_3) to promote the generation of volatile substances, as follows:

$$Cd^{2+}+e/e_{aq}/\cdot H/\cdot CH_3/...\rightarrow Cd^0 \quad (1)$$

$$Cd^{2+}+e/e_{aq}/\cdot H/\cdot CH_3/...\rightarrow CdH_2+CH_3\text{-}Cd\text{-}CH_3 \quad (2)$$

Hence, while the solvation of electrons is consumed during the decomposition of organic compounds, the resulting decomposition products can facilitate the production of volatile substances. Consequently, there is a certain level of promotion. Moreover, this promoting effect is particularly notable for elements such as Cd (as well as Hg) that are prone to generating volatile compounds via photochemical vapor generation (PVG).

Although the signal suppression mechanism of organic acids was not discussed in the Pan's work,[46] the ionized H^+ may play a crucial role. Formic acid and acetic acid are weak electrolyte acids, forming hydrogen ions in solution. The ionized H^+ might induce the formation of hydrogen and compete with the electrochemical reaction of the analyte.[30] That is to say, in addition to the decomposition of organic compounds, it should be noted that the ionization of organic acids can also lead to the depletion of solvated electrons, thus impeding the generation of volatile substances. Similarly, no signal enhancement was observed in Fig. 5c with the addition of formic acid and acetic acid, while methanol, ethanol, and propionic acid boosted Hg signals due to the potential promotion of the formation of mercury volatile substances by the aforementioned intermediates.[46] On closer inspection, the findings in the pH optimization experiment (Fig. 2a) reveals that H^+ ions exert a much stronger inhibitory effect on Ag and Cd compared to Hg. As a result, organic acids have demonstrated limited signal inhibitory effects on Hg (with a signal attenuation of 12% in the presence of 10 wt% formic acid, pH≈1.5), while they have a notable impact on the other two elements (with a signal attenuation of 88% and 92% induced by 10 wt% formic acid on Ag and Cd, respectively, pH≈1.5).

The effect of surfactants on the metal determination in SCGD-OES procedures has been noticed and proposed by different research groups.[38-39] But it is not clear that surfactants have helpful effects on analyte response of SAGD. Therefore, the effects of nonionic surfactant (Triton X-45, Triton X-100 and Triton X-405) on the emission intensity of Ag, Cd and Hg were studied. A series of Ag, Cd and Hg standard solutions containing 0.005, 0.01, 0.02 and 0.05 wt% of one of the above organic additives were prepared for test. The plasma can withstand the higher content of 0.1 and 0.2 wt% Triton X-405 existing in the solution. The results in Fig. 6 suggest that such surfactants are more favorable to analytes radiation than small organic molecules.

Fig. 8 The photograph of the SAGD plasma generated in contact with HNO_3 solution containing 0.05 wt% Triton X-405 (b), Triton X-100 (c) and Triton X-45 (d) or without surfactant (a).

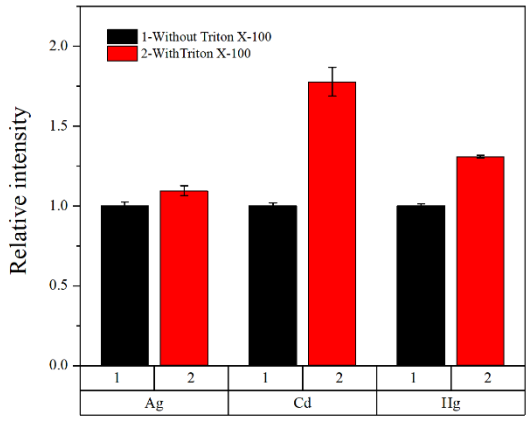

Fig. 9 The relative signals of Ag, Cd, and Hg in SAGD-ICP-OES before and after the addition of Triton X-100 (0.02 wt%).

On the premise of stable discharge, no obvious suppression of the signal was observed. Especially for Ag, the analyte response rises with surfactant content up, to 3.3 times of the initial signal when 0.2 wt% Triton X-405 was added. Cadmium and mercury signal improvement also occurred within the range of 0-0.02 wt% concentration (0-0.05 wt% for Triton X-405) and achieved optimal enhancement factors of 1.4 and 1.6 by addition of 0.02 wt% Triton X-100.

The pattern of emission spectra of the SAGD source generated in contact with nitric acid solution containing surfactant and solution without surfactant was found to differ over the spectral range of 200-400 nm (Fig. 7). Especially in the range of 200-270 nm, that is, the (2-0), (1-0), (0-0), (0-1), (0-2) and (0-3) bands of the third positive $A^2\sum^+ \rightarrow X^2\prod$ system containing NO molecules (band heads at 205.3, 215.5, 226.9, 237.0, 247.9 and 259.6 nm respectively), completely disappear or significantly decrease in the SAGD emission spectra generated with the addition of the Triton X series to the solution anode. The drop was most obvious and covered the entire spectrum in the case of Triton X-45 addition. Therefore, the addition of Triton X reagent can not only improve the signal intensity of the analyte, but also reduce the background radiation, thus improving the signal-to-back ratio (SBR).

Li *et al*.[47] found that the self-organized pattern formed on solution anode surface shows a bright disk under long camera exposure, and its diameter increases with the increase of discharge current. These results are roughly similar to our findings. The spot of the anode extended to the edge of the capillary outlet, and even spilled over when the current increases to 28 mA; as shown in Fig. 8a (see within the yellow dashed box), luminescence also occurs from the outlet to the lower part near it. Recent reports have suggested that the solute of anode solution significantly affects the formation of patterns.[48] The shrinkage of anode spot was observed in the presence of surfactant; see Figs. 8b, 8c and 8d, no light occurs down close to the outlet, and the light spot was also seen within the orifice edge with naked eyes. The glow discharge above the solution anode is abundant with electronegative substances, including NO and OH.[47, 49] Therefore, the reduction of these molecular bands may relate to the narrowed anode glow region with the contraction of the anode spot.

An assessment was conducted to evaluate the influence of Triton X-100 using the SAGD-ICP-OES method on the efficiency of elemental vapor generation, as discussed in the "The influence of salinity" section. To normalize the obtained signal, the signal of each element before the addition of Triton X-100 was defined as 1. The results (Fig. 9) indicated that Triton X-100 improved the transport efficiency of analyte, which provides one explanation for the observed increase in SAGD-OES signal. Note that the enhancement factors of SAGD-OES and SAGD-ICP-OES are inconsistent or even uncorrelated. This implies that the enhancement in analyte transport efficiency is not the sole contributing factor. Upon visual observation alongside spectra recordings (Figs. 7 and 8), significant changes were noticed in both the appearance of the plasma and background radiation. These finding suggests Triton X-100 has the possibility of influencing the element excitation, which may be related to the excitation position. The optimal collection optical path for Ag was found differed from

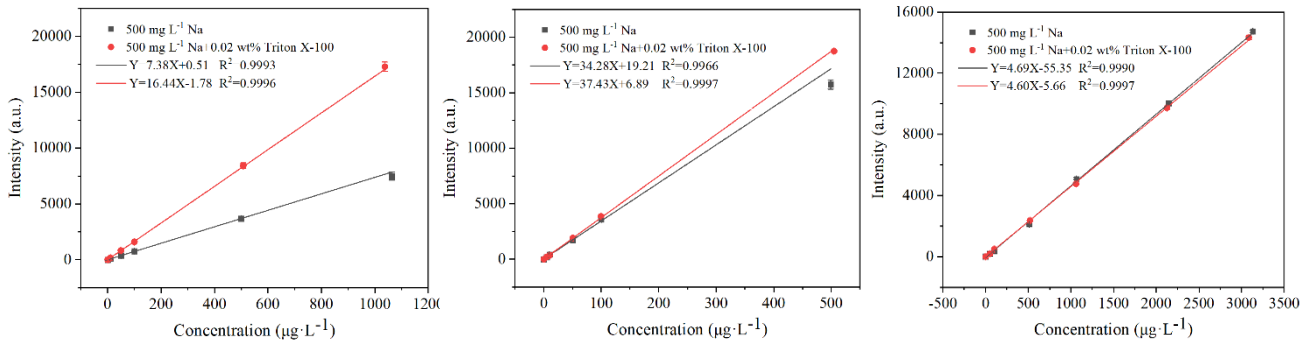

Fig. 10 Calibration curves established using the emission lines of Ag (a), Cd (b) and Hg (c) with or without the addition of Triton X-100 at a certain salinity.

Table 1. DLs of SAGD with/without Triton X-100 at a salinity of 500 mg L^{-1} Na, and comparisons with previously reported methods for Ag, Cd and Hg measurement

Method	Ag		Cd		Hg	
	DL (μg L^{-1})	Ref.	DL (μg L^{-1})	Ref.	DL (μg L^{-1})	Ref.
SAGD-OES	0.1	This work	0.2	This work	6	This work
SAGD-OES[a]	2.5	This work	1.2	This work	11	This work
SAGD-OES[b]	1.0	This work	0.9	This work	7	This work
SAGD-OES	0.03	6	0.07	6	1.7	6
SCGD-OES	2	7	7	7	92	7
LAGD-OES	-	-	-	-	11.3	32
LCGD-OES	-	-	13	50	350	51
FLA-APGD-OES	1.0	40	2.2	40	-	-
FLA-APGD-OES[c]	0.055 (0.004)[d]	5	0.049 (0.04)[d]	5	2.4 (0.7)[d]	5
FLC-APGD-OES	1.1	5	2.3	5	86	5
ICP-OES	5	Agilent 725[e]	5	Agilent 725[e]	18	Agilent 725[e]
WHO	-	-	3	52	6	52

LAGD: liquid anode glow discharge; LCGD: liquid cathode glow discharge.
[a] Solution contains 500 mg L^{-1} Na.
[b] Solution contains 500 mg L^{-1} Na and 0.02 wt% Triton X-100.
[c] Cathode rod is equipped with a water-cooled block.
[d] DLs are obtained for a system with the reduced background shift interferences.
[e] Agilent 725 manufacturer data.

that of the other two elements, which means distinct regions with the strongest excitation for Ag and the others. Overall, based on the current experimental results, it is challenging to accurately explain the effects of Triton X-100, as they cannot be attributed to a single mechanism. Further research utilizing more detailed experiments and advanced diagnostic techniques will be beneficial in gaining deeper insights into this phenomenon.

Analytical calibration in the presence of 500 mg L^{-1} Na. A series of standard solutions, containing one of the three selected elements (Ag, Cd and Hg), covering concentration ranges of 10-1000 μg L^{-1} (for Ag), 5-500 μg L^{-1} (for Cd) or 50-3000 μg L^{-1} (for Hg), were analyzed at Na concentration of 500 mg L^{-1} to elaborate calibration curves under optimized operating conditions. The addition of 0.02 wt% Triton X-100 to the test solution was considered advantageous for the measurement, and thus the effect of Triton X-100 on salt substrates was also investigated, due to the fact that standard addition methods were common in SAGD-OES procedure. A series of standard solutions, composed of 0.02 wt% Triton X-100, 500 mg L^{-1} Na and one of the selected element (5-1000 μg L^{-1} of Ag, 5-500 μg L^{-1} of Cd or 20-3000 μg L^{-1} of Hg), were also prepared and analyzed.

Figure. 10 shows the calibration curves for each analyte in the selected concentration range with or without the addition of Triton X-100. Apparent declines in the background level were still found to occur for Triton X-100 in a salt environment (500 mg L^{-1} Na), and better SBRs were derived. And show from chart: the performance of linearity was improved using Triton X-100 (see R^2 in the linear equations). Triton X-100 still guaranteed a ≥ 2-fold increase in Ag response (see the slope of the linear equations), and the presence or absence of 500 mgL^{-1} Na in the electrolyte has little effect. For Cd and Hg, great amount natrium salt weakens or even eliminates the positive effect of Triton X-100, but fortunately there is no inhibition. From the perspective of detection limit (DL, DL=3 SD/s, SD is the standard deviation of 11 blank measurements, and s is the slope of the calibration curve), Triton X-100 treated sample solution is highly worth considering in the

Table 2. The results of the determination of Ag, Cd and Hg in tap-water and mineral water samples with the addition of 0.02 wt% Triton X-100. (n=3, ±SD)

Sample	Element	Add (μg L^{-1})	Found (μg L^{-1})	Recovery (%)
Tap-water	Ag	10.0	9.76 ± 0.51	97.6
	Cd	10.0	10.4 ± 0.8	104
	Hg	50.0	49.8 ± 4.1	99.6
Mineral water	Ag	10.0	9.40 ± 0.15	94.0
	Cd	10.0	10.2 ± 0.1	102
	Hg	50.0	51.1 ± 3.5	102

determination method based on the SAGD-cell designed here, accompanied by the improvement of DLs for three elements. Table 1 summarizes the DLs of SAGD-OES with/without Triton X-100 at a certain salinity (500 mg L^{-1} Na), as well as a comparison with previously reported Ag, Cd, and Hg determination methods. For a fairer comparison, no inert gas, water-cooled block, or special sample introduction unit was used in all other microplasma spectral measurements. This method presented herein exhibits superior detection limits, even with 500 mg L^{-1} Na.

In order to verify the applicability of the developed method, the recoveries assessed for Ag, Cd, and Hg added to tap-water and mineral water were quantitative in the presence of Triton X-100. The results shown in Table 2 indicate that the method presented is of great exactness, with recoveries ranging between 94% and 104%.

CONCLUSION

After a study on the influence of the nitrate and organic additive content on the analytical performance of a SAGD-OES system, the following conclusions were obtained: (1) the influence of salt matrix on analytes varies greatly, and overall, the signal of Ag is suppressed the most, followed by Cd and finally Hg; (2) the standard addition method is preferred in the determination of Ag and Cd, while the simple standard curve method can be used for Hg, given its gratifying recovery rate with 100 mg L^{-1} coexisting ions; (3) organic small molecules exhibit controversial performance—LMWOCs only favor the emission of mercury and on the contrary, the signals of Ag and Cd are not enhanced or even restrained; (4) surfactants such as Triton X series can not only boost the emission signal of analytes but also reduce the background level, with Ag, Cd and Hg responses increasing by up to 3.3-, 1.4- and 1.6- fold, respectively; (5) the use of additives in sodium nitrate matrices is also efficient, since SBRs, DLs and linearity performance are normally improved.

The conclusions above provide some suggestions for the analysis of samples containing a certain salt matrix. For instance, using surfactants like Triton X-100. However, the cause and mechanism of matrix induced interference are not fully understood. According to the current research, the presence of $Na^+/K^+/Mg^{2+}/Ca^{2+}$ neither significantly affect the plasma parameters nor caused any spectral interferences. Therefore, it can be inferred that the electrochemical process of analyte entering the plasma is vital, but such transient process is hard to be clearly recognized and explained. In-depth research will also be conducted in the future work, with the development of diagnostic techniques and approaches.

AUTHOR INFORMATION

Zheng Wang received his PhD in 2006 from the Shanghai Institute of Ceramics, Chinese Academy of Sciences (CAS). He is a research professor and PhD supervisor at the Shanghai Institute of Ceramics, CAS. His major research interests are environmental analytical chemistry, spectroscopy instrument development, preparation and characterization of new inorganic materials, 3D printing materials and precision manufacturing, etc. He has been working as member of editorial board for *Atomic Spectroscopy*, *Chinese Chemical Letters,* and *Spectroscopy and Spectral Analysis*. Zheng Wang is author or co-author of over 100 articles published in peer-reviewed scientific journals. In 2010 and 2018, he received two science and technology awards from the China Association for Analysis and Testing.

Corresponding Author

*Z. Wang

Email address: wangzheng@mail.sic.ac.cn

Notes

The authors declare no competing financial interest.

ACKNOWLEDGMENTS

This work was supported by the Science and Technology Innovation Plan of Shanghai Science and Technology Commission (22DZ2201700), the National Natural Science Foundation of China (12105354), and the Shanghai Technical Platform for Testing and Characterization on Inorganic Materials (19DZ2290700).

REFERENCES

1. Y.R. Zhang, J.X. Liu, X.F. Mao, G.Y. Chen, and D. Tian, *TrAC-Trend. Anal. Chem.*, 2021, **144**, 116437. https://doi.org/10.1016/j.trac.2021.116437

2. J. Hu, C.H. Li, Y.F. Zhen, H.J. Chen, J. He, and X.D. Hou, *TrAC-Trend. Anal. Chem.*, 2022, 155, 116677. https://doi.org/10.1016/j.trac.2022.116677
3. X.X. Peng and Z. Wang, *Chinese Chem. Lett.*, 2022, 33, 61–70. https://doi.org/10.1016/j.cclet.2021.06.017
4. M. Gorska, K. Greda, and P. Pohl, *J. Anal. At. Spectrom.*, 2021, **36**, 165–177. https://doi.org/10.1039/d0ja00401d
5. K. Greda, K. Swiderski, P. Jamroz, and P. Pohl, *Anal. Chem.*, 2016, 88, 8812–8820. https://doi.org/10.1021/acs.analchem.6b02250
6. M. L. Yuan, X. X. Peng, F. Ge, Q. Li, K. Wang, D. G. Yu, and Z. Wang, *Microchem. J.*, 2020, **155**, 104785. https://doi.org/10.1016/j.microc.2020.104785
7. X. X. Peng, X. H. Guo, F. Ge, and Z. Wang, *J. Anal. At. Spectrom.*, 2019, **34**, 394–400. https://doi.org/10.1039/c8ja00369f
8. K. Świderski, P. Pohl, and P. Jamróz, *J. Anal. At. Spectrom.*, 2019, **34**, 1287–1293. https://doi.org/10.1039/c9ja00038k
9. K. Swiderski, K. Greda, P. Pohl, and P. Jamroz, *J. Anal. At. Spectrom*., 2022, **37**, 517–527. https://doi.org/10.1039/d1ja00433f
10. K. György, L. Bencs, P. Mezei, and T. Cserfalvi, *Spectrochim. Acta B*, 2012, **77**, 52–57. https://doi.org/10.1016/j.sab.2012.09.002
11. N. Hazel, J. Orejas, and S. J. Ray, *Spectrochim. Acta B*, 2021, **176**, 106040. https://doi.org/10.1016/j.sab.2020.106040
12. Z. Q. Cai, L. Qian, X. X. Peng, and Z. Wang, *Anal. Chem.*, 2021, **93**, 14701–14707. https://doi.org/10.1021/acs.analchem.1c03057
13. C. Yang, D. He, Z. L. Zhu, H. Peng, Z. F. Liu, G. J. Wen, J. H. Bai, H. T. Zheng, S. H. Hu, and Y. X. Wang, *Anal. Chem.*, 2017, **89**, 3694–3701. https://doi.org/10.1021/acs.analchem.6b05158
14. X. X. Peng and Z. Wang, *Anal. Chem.*, 2019, **91**, 10073–10080. https://doi.org/10.1021/acs.analchem.9b02006
15. R. Rong, Z. Q. Cai, X. Y. Li, and Z. Wang, *J. Anal. At. Spectrom.*, 2022, **37**, 2377–2382. https://doi.org/10.1039/D2JA00257D
16. J. H. Dong, C. Yang, D. He, H. T. Zheng, S. H. Hu, and Z. L. Zhu, *Atom. Spectrosc.*, 2020, **41**, 57–63. https://www.at-spectrosc.com/as/article/pdf/202002002?st=article_issue
17. A. Q. Leng, Y. F. Tian, M. X. Wang, L. Wu, K. L. Xu, X. D. Hou, and C.B. Zheng, *Chinese Chem. Lett.*, 2017, **28**, 189–196. https://doi.org/10.1016/j.cclet.2016.06.056
18. N. Li, Z. C. Wu, Y. Y. Wang, J. Zhang, X. N. Zhang, H. N. Zhang, W.H. Wu, J. Gao, and J. Jiang, *Anal. Chem.*, 2017, **89**, 2205–2210. https://doi.org/10.1021/acs.analchem.6b03523
19. M. T. Li, Y. Luo, Z. R. Zou, F. J. Xu, X. M Jiang, and X. D. Hou, *J. Anal. At. Spectrom.*, 2021, **36**, 2735–2743. https://doi.org/10.1039/D1JA00290B
20. X. Yuan, K. J. Li, Y. T. Zhang, Y. T. Miao, Y. Xiang, Y. Sha, M. Zhang, and K. Huang, *Microchem. J.*, 2020, **155**, 104695. https://doi.org/10.1016/j.microc.2020.104695
21. Z. Q. Tan, B. W. Wang, Y. G. Yin, Q. Liu, X. Li, and J. F. Liu, *Anal. Chem.*, 2020, **92**, 1549–1556. https://doi.org/10.1021/acs.analchem.9b04837
22. J. H. Yang, Y. Lin, L. B. He, Y. B. Su, X. D. Hou, Y. R. Deng, and C. B. Zheng, *Anal. Chem.*, 2021, **93**, 14923–14928. https://doi.org/10.1021/acs.analchem.1c02023
23. L. He, P. X. Li, K. Li, T. Lin, J. Luo, X. D. Hou, and X. M. Jiang, *J. Anal. At. Spectrom.*, 2021, **36**, 1193–1200. https://doi.org/10.1039/D1JA00039J
24. Y. B. Su, X. M. Pan, Y. Lin, Y. R. Deng, and C. B. Zheng, *Atom. Spectrosc.*, 2023, **44**, 76–83. https://doi.org/10.46770/as.2023.091
25. T. Cserfalvi and P. Mezei, *J. Anal. At. Spectrom.*, 1994, **9**, 345–349. https://doi.org/10.1039/ja9940900345
26. T. Cserfalvi, P. Mezei, and P. Apai, *J. Phys. D Appl. Phys.*, 1993, **26**, 2184–2188. https://doi.org/10.1088/0022-3727/26/12/015
27. X. Liu, Z. L. Zhu, D. He, H. T. Zheng, Y. Q. Gan, N. S. Belshaw, S. H. Hu, and Y. X. Wang, *J. Anal. At. Spectrom.*, 2016, **31**, 1089–1096. https://doi.org/10.1039/c6ja00017g
28. K. Greda, M. Gorska, M. Welna, P. Jamroz, and P. Pohl, *Talanta*, 2019, **199**, 107–115. https://doi.org/10.1016/j.talanta.2019.02.058
29. Z.Q. Cai and Z. Wang, *Spectrochim. Acta B*, 2023, **199**, 106578. https://doi.org/10.1016/j.sab.2022.106578
30. C. Yang, G. Cheng, S. Q. Cheng, X. Liu, Y. Liu, H. T. Zheng, S. H. Hu, and Z. L. Zhu, *Anal. Chem.*, 2021, **93**, 16393–16400. https://doi.org/10.1021/acs.analchem.1c02940
31. Y. Liu, C. Yang, P. J. Xing, X. Liu, J. Z. Liu, and Z. L. Zhu, *J. Anal. At. Spectrom.*, 2023, **38**, 742–750. https://doi.org/10.1039/D2JA00382A
32. J. Yu, L. J. Cui, Q. F. Lu, J. L. Li, Y. Feng, B. Wang, and X. J. Ma, *Spectrochim. Acta B*, 2021, **186**, 106311. https://doi.org/10.1016/j.sab.2021.106311
33. K. Greda, A. Szymczycha-Madeja, and P. Pohl, *Anal. Chim. Acta*, 2020, **1123**, 81–90. https://doi.org/10.1016/j.aca.2020.05.026
34. M. Gorska, P. Pohl, and K. Greda, *Microchem. J.*, 2021, **164**, 105975. https://doi.org/10.1016/j.microc.2021.105975
35. J. Yu, Y. J. Kang, Q. F. Lu, H. Luo, Z. H. Lu, L. J. Cui, and J. L. Li, *Microchem. J.*, 2020, **159**, 105507. https://doi.org/10.1016/j.microc.2020.105507.
36. R. Manjusha, M. A. Reddy, R. Shekhar, and S. Jaikumar, *J. Anal. At. Spectrom.*, 2013, **28**, 1932–1939. https://doi.org/10.1039/c3ja50202c
37. C. G. Decker and M. R. Webb, *J. Anal. At. Spectrom.*, 2016, **31**, 311–318. https://doi.org/10.1039/c5ja00243e
38. K. Greda, P. Jamroz, and P. Pohl, *J. Anal. At. Spectrom.*, 2013, **28**, 134–141. https://doi.org/10.1039/c2ja30275f
39. Z. Zhang, Z. Wang, Q. Li, H. J. Zou, and Y. Shi, *Talanta*, 2014, **119**, 613–619. https://doi.org/10.1016/j.talanta.2013.11.010
40. K. Swiderski, A. Dzimitrowicz, P. Jamroz, and P. Pohl, *J. Anal. At. Spectrom.*, 2018, **33**, 437–451. https://doi.org/10.1039/c7ja00374a
41. K. Greda, S. Burhenn, P. Pohl, and J. Franzke, *Talanta*, 2019, **204**, 304–309. https://doi.org/10.1016/j.talanta.2019.06.015
42. Z. Q. Cai and Z. Wang, *Anal. Chim. Acta*, 2022, **1203**, 339724. https://doi.org/10.1016/j.aca.2022.339724
43. Y. Zhang, J. Orejas, J. Fandiño, D. Blanco Fernández, J. Pisonero, and N. Bordel, *J. Anal. At. Spectrom.*, 2022, **37**, 1150–1160. https://doi.org/10.1039/D1JA00439E
44. Z. Wang, R. Y. Gai, L. Zhou, and Z. Zhang, *J. Anal. At. Spectrom.*, 2014, 29, 2042–2049. https://doi.org/10.1039/C4JA00173G
45. K. Greda, M. Welna, A. Szymczycha-Madeja, and P. Pohl, *Talanta*, 2022, **249**, 123694. https://doi.org/10.1016/j.talanta.2022.123694
46. X. M. Pan, Y. Lin, Y. B. Su, J. H. Yang, L. B. He, Y. R. Deng, X. D. Hou, and C. B. Zheng, *Anal. Chem.*, 2021, **93**, 8257–8264. https://doi.org/10.1021/acs.analchem.1c01091

47. X. C. Li, P. C. Kang, K. Gao, S. Zhou, K. Y. Wu, and P. Y. Jia, *Plasma Process. Polym.*, 2020, **17**, 1900223. https://doi.org/10.1002/ppap.201900223
48. T. Srivastava, M. S. Simeni, G. Nayak, and P. J. Bruggeman, *Plasma Sources Sci. Technol*., 2022, **31**, 085010. https://doi.org/10.1088/1361-6595/ac83ed
49. K. Y. Wu, N. Zhao, Q. M. Niu, J. C. Wu, S. Zhou, P. Y. Jia, and X. C. Li, *Plasma Sci. Technol*., 2022, **24**, 055405. https://doi.org/10.1088/2058-6272/ac48e1
50. Q. F. Lu, F. F. Feng, J. Yu, L. Yin, Y. J. Kang, H. Luo, D. X. Sun, and W. Yang, *Microchem. J*., 2020, **152**, 104308. https://doi.org/10.1016/j.microc.2019.104308
51. J. Yu, L. Yin, Q.F. Lu, F. F. Feng, Y. J. Kang, and H. Luo, *Anal. Chim. Acta*, 2020, **1131**, 25–34. https://doi.org/10.1016/j.aca.2020.07.050
52. WHO, Guidelines for Drinking Water Quality, 4th Edition. World Health Organization: Geneva, Switzerland, 2020.